

ARGONNE NATIONAL LABORATORY
9700 South Cass Avenue
Lemont, Illinois 60439

**Photoinjector Optimization using a Derivative-Free,
Model-Based Trust-Region Algorithm for the Argonne
Wakefield Accelerator**

Nicole Neveu, Jeffrey Larson, John G. Power, and Linda Spentzouris

Mathematics and Computer Science Division

Preprint ANL/MCS-P7041-0417

April 2017

¹This material is based upon work supported by the U.S. Department of Energy, Office of Science, Office of Advanced Scientific Computing Research under contract number DE-AC02-06CH11357.

PHOTOINJECTOR OPTIMIZATION USING A DERIVATIVE-FREE, MODEL-BASED TRUST-REGION ALGORITHM FOR THE ARGONNE WAKEFIELD ACCELERATOR

N. Neveu,^{1,2*} J. Larson,¹ J. G. Power,¹ L. Spentzouris,²

¹Argonne National Laboratory, Lemont, IL and ²Illinois Institute of Technology, Chicago, IL

Abstract

Model-based, derivative-free, trust-region algorithms are increasingly popular for optimizing computationally expensive numerical simulations. A strength of such methods is their efficient use of function evaluations. In this paper, we use one such algorithm to optimize the beam dynamics in two cases of interest at the Argonne Wakefield Accelerator (AWA) facility. First, we minimize the emittance of a 1 nC electron bunch produced by the AWA rf photocathode gun by adjusting three parameters: rf gun phase, solenoid strength, and laser radius. The algorithm converges to a set of parameters that yield an emittance of 1.08 μm . Second, we expand the number of optimization parameters to model the complete AWA rf photoinjector (the gun and six accelerating cavities) at 40 nC. The optimization algorithm is used in a Pareto study that compares the trade-off between emittance and bunch length for the AWA 70 MeV photoinjector.

THE AWA FACILITY

The 70 MeV rf photoinjector at the Argonne Wakefield Accelerator (AWA) facility [1] consists of an rf gun followed by six rf accelerating cavities, hereafter referred to as the linac. See Fig. 1 for the beam line layout. The 1.5 cell rf gun operates at 1.3 GHz with three solenoids and a Cs₂Te photocathode excited by a 248 nm UV laser. Solenoid 1 (S_1) is used to buck the field at the cathode, while the other two solenoids (S_2 and S_3) are used for emittance compensation. The accelerating cavities, also operated at 1.3 GHz, are 7 cell standing-wave cavities [2] each with independently controllable phase. The cavities are labeled L_1 - L_6 in Fig. 1.

OPTIMIZATION ALGORITHM

Model-based, derivative-free algorithms are frequently used to optimize computationally expensive simulations due to their judicious use of function evaluations. In cases specific to accelerator physics, beam properties at different operational parameters are observed; these methods then build models of the unknown function and minimize these models to identify candidate parameters to evaluate. BOBYQA [3] is one such method that is available via the NLOpt [4] package and was used in this study. Given a candidate set of optimal parameters v^k , BOBYQA constructs a quadratic model using function values of points near v^k . This model is minimized in a neighborhood of v^k in order to produce a point \hat{v} . If \hat{v} has a smaller objective function value than v^k ,

the estimate of the optimum is updated to \hat{v} , and a new model is constructed. If \hat{v} is not a sufficient improvement over v^k , the model around v^k is improved. For more information about derivative-free optimization, see [5].

The parameters v^k are generated and supplied to the open source particle-in-cell code OPAL-T [6]. This code was chosen in part because it models the 3D space charge necessary to accurately simulate of the linac. The optimization package NLOpt and OPAL-T were used in combination with Python code written at Argonne National Laboratory to perform simulation evaluations and optimization. All the files needed to replicate the results in this paper are available at

www.mcs.anl.gov/~jlarson/AWA.

Interested parties are welcome to adapt the code to their needs and suggest improvements.

OPTIMIZATION PARAMETERS

When optimizing the gun, three parameters were varied: solenoid strength (S_3), gun phase (ϕ_g), and laser radius (R) of a uniform pulse. The minimized objective was emittance (ϵ_x). (The phase is defined as 0° at maximum energy gain.) When optimizing the entire linac, seven additional parameters were varied: the longitudinal laser full width at half maximum (T) and accelerating cavity phases (ϕ_L). The optimization parameters and bounds are given in Table 1; we denote the set of ten optimization parameters as $v = [S_3, \phi_g, R, T, \phi_L]$, where $\phi_L = [\phi_{L_1}, \dots, \phi_{L_6}]$ represents the phase of each linac cavity L_1 - L_6 .

Table 1: Bounds on Parameters for Gun and Linac Optimization

Variable	Range	Unit
Solenoid Strength	$0 \leq S_3 \leq 440$	amps
Phase of Gun	$-60 \leq \phi_g \leq 60$	degrees
Laser Radius	$3 \leq R \leq 15$	mm
Laser FWHM ¹	$2 \leq T \leq 10$	ps
Cavity Phase ¹	$-20 \leq \phi_L \leq 20$	degrees

¹ not varied during gun optimization

GUN OPTIMIZATION

Much work has been done to optimize 1.5 cell rf guns at 1 nC [7]. This known solution was used as a baseline test of BOBYQA when applied to an accelerator application. An optimization of the single objective emittance (ϵ_x)

* nneveu@hawk.iit.edu

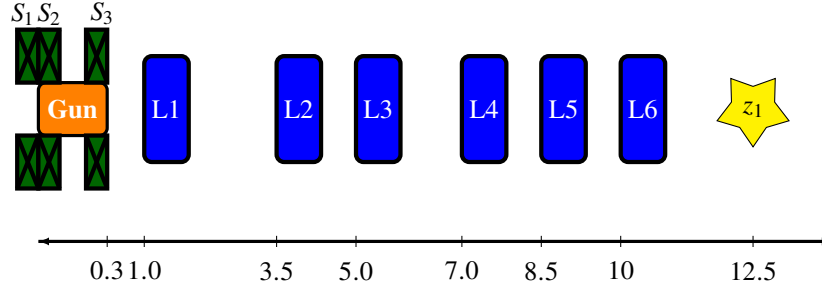


Figure 1: Layout of the AWA linac. The gun is enlarged to show solenoid detail. The physical length is 0.3 m. The cathode is located at $z = 0$ m. Linac cavities are 0.85 m long. Tick marks are located at the exit of the gun, entrance of each accelerating cavity, and location of optimization.

was performed over a length of 5 m. All linacs were turned off and only gun parameters were varied. Nonvarying parameters are listed in Table 2; their values are based on work done at PITZ and AWA [7, 8]. Local optimization runs were started from five points with various distances from the optimum value. The optimization runs converged (in less than 100 function evaluations) to a parameter set ($M = 269$, $\phi_g = -3.0$, and $R = 0.0006$) with an emittance of $1.08 \mu\text{m}$. An exhaustive search of the parameter space was not done, and there may be other local minima that were not found. However, the results match expectations based on the literature.

Table 2: Nonvarying Parameters for Gun Optimization

Parameter	Value
Charge	1 nC
Gradient	60 MV/m
Laser FWHM	20 ps
Laser Rise and Fall Time	6 ps
Kinetic Energy at Cathode	0.55 eV
S_1 and S_2	550 A

LINAC OPTIMIZATION

Next we performed a multiobjective optimization of the linac (Fig. 1), by adjusting the ten parameters in Table 1. The charge was set to 40 nC and was chosen for upcoming two-beam acceleration experiments [9]. Two objectives were considered: emittance, and bunch length, σ_z . The location of interest is $z_1 = 12.51$ m, as this is the entrance of the first quadrupole magnet after the linac. We optimize ϵ_x instead of ϵ_{xy} because no asymmetric focusing elements were used in the linac. The nonvarying parameters for all linac simulation runs are shown in Table 3. The model used simulated emission from a Cs₂Te cathode using a laser with initial kinetic energy of 4 eV. These are typical operating conditions at AWA.

A 1,000 point sample of linac parameters were drawn uniformly from the domain in Table 1 and simulated. Of these, 132 simulations completed without error, and the

Table 3: Nonvarying Parameters for Linac Optimization

Parameter	Value
Charge	40 nC
Laser Rise and Fall Time	1.0 ps
Gun Gradient	70 MV/m
S_1 and S_2	550 A
Cavity Gradient 1–4	25 MV/m
Cavity Gradient 5–6	27 MV/m

emittance and bunch length at $z_1 = 12.51$ m was recorded for each of these points, p_i . The raw ϵ_x and σ_z values were then shifted and scaled to produce $\bar{\epsilon}_x$, and $\bar{\sigma}_z$, which have a minimum value of 0 and a maximum value of 1 over the 132-point sample set. This scaling is done in order to remove the difference in the units between emittance and bunch length when optimizing.

With the scaled values of $\bar{\epsilon}_x$ and $\bar{\sigma}_z$, a sequence of eleven optimization problems were solved by minimizing

$$f(v, w) = w \bar{\epsilon}_x(v, z_1) + (1 - w) \bar{\sigma}_z(v, z_1), \quad (1)$$

for $w \in \{0, 0.1, 0.2, \dots, 1\}$. For each weight w , BOBYQA was started from the sample point with the smallest value of $f(v, w)$. From the initial random sample, six unique starting points were chosen. (There were fewer starting points than weights because some samples, p_i , had the smallest result for multiple weights. For example, sample p_{18} had the smallest result for three objectives, $f(v, 0.4)$, $f(v, 0.5)$, and $f(v, 0.6)$.)

PARETO FRONT FOR AWA LINAC

Since multiple objectives are under consideration in this case, a trade-off analysis is necessary. This can be aided by examining a Pareto front: the set of parameters for which no other point exists that is better with respect to both objectives [10]. In Fig. 2, blue dots show the emittance and bunch length for the evaluated random sample. The sample points for which no other point has better emittance and bunch length are connected with a blue line. BOBYQA was

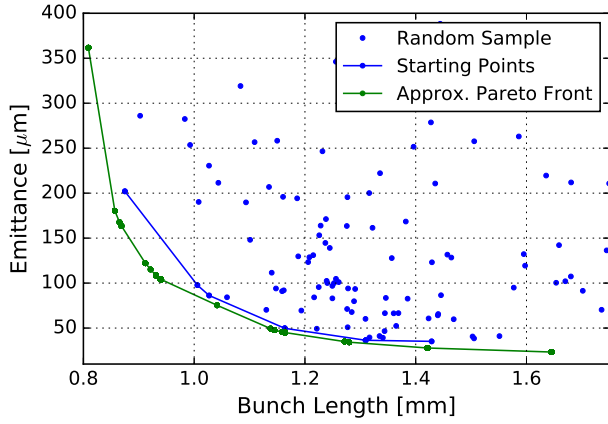


Figure 2: Random sample results, starting sample points, and resulting approximate Pareto front for the linac at 40 nC. The Pareto front is the result of all BOBYQA evaluations.

started from these points, as described above, producing the green approximate Pareto front.

The number of simulation evaluations needed to obtain convergence in the BOBYQA runs varied from a minimum of 107 evaluations to a maximum of 208 evaluations. In order to generate the Pareto front in Fig. 2, a total of 2,492 simulation evaluations were completed. The best-found objective value through each BOBYQA run is shown in Fig. 3. We note that most of the BOBYQA runs converged to emittance values between 20 μm and 45 μm , and many of the optimized points had negative phases for L_1 and L_2 . This is interesting since the AWA does not typically operate with such parameters. We suspect the negative phases in the linac are compensating for the initial energy spread out of the gun. Physical experiments will be conducted to test this new configuration.

Figure 4 shows the gun phase and laser full width at half maximum at each of the eleven optimized points. We annotate Fig. 4 with T because that parameter shows strong correlation with the gun phase. Other optimized parameters

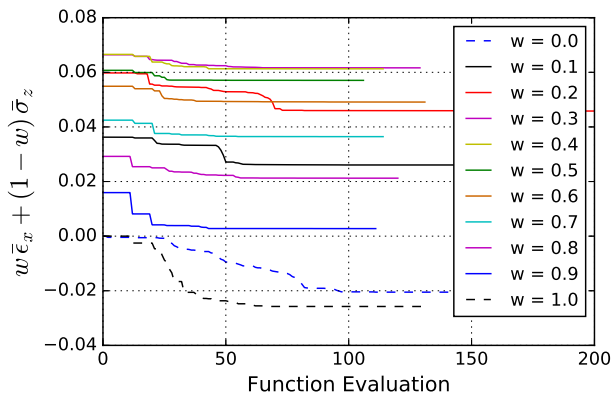


Figure 3: Minimum observed objective function values during eleven BOBYQA runs at 40 nC.

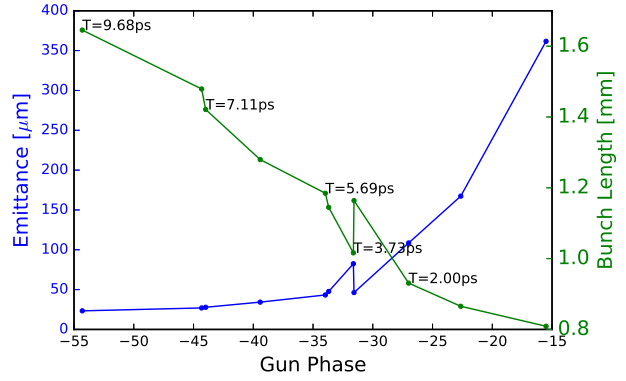


Figure 4: Bunch length and emittance vs. gun phase at each optimized point in the Pareto front for the linac at 40 nC. The phase of the maximum energy gain is 0°.

such as the laser radius were found to stay within a narrow range (10 mm–14 mm). We speculate the discontinuity around -30° may be a result of sensitivity to numerical noise in a region where the emittance is changing quickly.

CONCLUSION

Using an AWA beam line as the simulation model, we used the BOBYQA algorithm to optimize the emittance produced by the gun at 1 nC. Using the same algorithm, we performed a multiobjective analysis for the linac at 40 nC. A Pareto front comparing the trade-off between bunch length and emittance was generated for the linac. This analysis will be used to decide future operating parameters at the AWA during high-charge experiments. In total, only 2,492 simulation evaluations were needed to produce the approximate Pareto front.

Future work will include a refinement of results using 3D field maps for all cavities, experimental measurements to verify the Pareto front, and a comparison with evolutionary algorithms.

ACKNOWLEDGMENT

We gratefully acknowledge the computing resources provided on Blues, a high-performance computing cluster operated by the LCRC at Argonne National Laboratory. This material is based upon work supported by the U.S. Department of Energy, Office of Science, under contract numbers DE-AC02-06CH11357, DE-AC02-06CH11357, and grant number DE-SC0015479.

REFERENCES

- [1] M. Conde *et al.*, “Research program and recent results at the Argonne Wakefield Accelerator facility (AWA),” in *Proc. IPAC’17*, Copenhagen, Denmark, May 2017, paper WEPAB132.
- [2] J. Power, M. Conde, W. Gai, Z. Li, and D. Mihalcea, “Upgrade of the drive LINAC for the AWA facility dielectric

- two-beam accelerator,” in *Proc. IPAC’10*, Kyoto, Japan, May 2010, paper THPD016.
- [3] M. Powell, “The BOBYQA algorithm for bound constrained optimization without derivatives,” University of Cambridge, U.K., Rep. NA2009/06, Oct. 2009.
 - [4] S. G. Johnson, “The NLOpt nonlinear-optimization package,” <http://ab-initio.mit.edu/nlopt>
 - [5] A. R. Conn, K. Scheinberg, and L. N. Vicente, *Introduction to Derivative-Free Optimization*. SIAM, 2009.
 - [6] A. Adelmann *et al.*, “The OPAL (Object Oriented Parallel Accelerator Library) framework,” PSI, Zurich, Switzerland, Rep. PSI-PR-08-02, 2008-2017.
 - [7] F. Stephan *et al.*, “Detailed characterization of electron sources yielding first demonstration of European X-ray free-electron laser beam quality,” *Phys. Rev. ST Accel. Beams*, vol. 13, p. 020704, 2010.
 - [8] N. Neveu *et al.*, “Benchmark of rf photoinjector and dipole using ASTRA, GPT, and OPAL”, in *Proc. NAPAC’16*, Chicago, IL, Oct. 2016, paper THPOA46.
 - [9] C. Jing *et al.*, “The two beam acceleration staging experiment at Argonne Wakefield Accelerator facility,” in *Proc. IPAC’15*, Richmond, VA, May 2015, paper WEPJE020.
 - [10] M. Ehrgott, *Multicriteria Optimization*. Berlin, Germany: Springer Science & Business Media, 2005.

The submitted manuscript has been created by UChicago Argonne, LLC, Operator of Argonne National Laboratory (“Argonne”). Argonne, a U.S. Department of Energy Office of Science laboratory, is operated under Contract No. DE-AC02-06CH11357. The U.S. Government retains for itself, and others acting on its behalf, a paid-up nonexclusive, irrevocable worldwide license in said article to reproduce, prepare derivative works, distribute copies to the public, and perform publicly and display publicly, by or on behalf of the Government. The Department of Energy will provide public access to these results of federally sponsored research in accordance with the DOE Public Access Plan. <http://energy.gov/downloads/doe-public-access-plan>.